Talanta 211 (2020) 120757

Contents lists available at ScienceDirect

Talanta

journal homepage: www.elsevier.com/locate/talanta

Simultaneous detection of salivary Δ^9-tetrahydrocannabinol and alcohol using a Wearable Electrochemical Ring Sensor

Rupesh K. Mishra[a,b,1], Juliane R. Sempionatto[a,1], Zhanhong Li[a], Christopher Brown[a], Nathalia M. Galdino[a], Rushabh Shah[a], Shuyang Liu[a], Lee J. Hubble[a,c], Kara Bagot[d,e], Susan Tapert[d], Joseph Wang[a,*]

[a] Department of Nanoengineering, University of California San Diego, La Jolla, CA 92093, USA
[b] Amity Institute of Biotechnology, Amity University Rajasthan, Jaipur, 303002, India
[c] CSIRO Manufacturing, Lindfield, New South Wales 2070, Australia
[d] Department of Psychiatry, University of California, San Diego, La Jolla, CA 92093, USA
[e] Department of Psychiatry, Addiction Institute of Mount Sinai, Icahn School of Medicine at Mount Sinai, New York, NY 10029, USA

ARTICLE INFO

Keywords:
Wearable THC sensor
Alcohol sensor
Marijuana sensor
Ring sensor
Saliva sensor
Electrochemical sensor

ABSTRACT

Driving under the influence of cannabis and alcohol represents a major safety concern due to the synergistic or additive effect of these substances of abuse. Hence, rapid road-site testing of these substances is highly desired to reduce risks of fatal accidents. Here we describe a wearable electrochemical sensing device for the simultaneous direct, decentralized, detection of salivary THC and alcohol. The new ring-based sensing platform contains a voltammetric THC sensor and an amperometric alcohol biosensor on the ring cap, along with the wireless electronics embedded within the ring case. Rapid replacement of the disposable sensing-electrode ring cap following each saliva assay is accomplished by aligning spring-loaded pins, mounted on the electronic board (PCB), with the current collectors of the sensing electrodes. The printed dual-analyte sensor ring cover is based on a MWCNT/carbon electrode for the THC detection along with a Prussian-blue transducer, coated with alcohol oxidase/chitosan reagent layer, for the biosensing of alcohol. THC and alcohol can thus be detected simultaneously in the same diluted saliva sample within 3 min, with no cross talk and no interferences from the saliva matrix. The new wearable ring sensor platform should enable law enforcement personnel to screen drivers in a single traffic stop and offers considerable promise for addressing growing concerns of drug-impaired driving.

1. Introduction

Alcohol and cannabis are the most commonly used psychoactive drugs, and they are often used in combination [1–4]. Driving under the influence of cannabis and alcohol is an increasing concern due to the synergistic or additive effect of both compounds. Unfortunately, the number of drivers using both cannabis and alcohol has increased dramatically in recent years. Recent reports have shown that over 10 million people in the United states have been driving under the impact of unlawful drugs over a year [5], and that 32% of the total fatalities from car crashes in the U.S.A in 2008 have been alcohol related [6]. Two thirds of the US trauma centre admissions are due to the motor vehicle accidents with almost 60% of such patients testing positive for drugs or alcohol [7]. Marijuana has been found to be the most prevalent drug detected in impaired drivers and motor vehicle crash victims [7–9]. Researchers have recently found that drivers who had consumed mixed alcohol and marijuana have double odds of suffering a fatal road accident [10–13]. Other studies show that collision risk, after mixing the substances, is four times greater than the risk of a person who used only one of the substances [14,15]. Cannabis, cocaine and methamphetamine are the drugs most frequently detected in drivers randomly stopped for roadside drug screening [16]. It is important to notice that driving impaired by any constituent, whether marijuana or alcohol, is illegal and against the law in the United states. With the recent legalization of recreational cannabis use, there are urgent needs to develop rapid, accurate and simple roadside tests that can detect Δ^9-tetrahydrocannabinol (THC), the main psychoactive ingredient in cannabis [17], in non-invasive body fluids alone or simultaneously with alcohol.

* Corresponding author.
E-mail address: josephwang@eng.ucsd.edu (J. Wang).
[1] Equal first author.

https://doi.org/10.1016/j.talanta.2020.120757
Received 3 December 2019; Received in revised form 8 January 2020; Accepted 16 January 2020
Available online 16 January 2020
0039-9140/

Existing roadside testing of suspected impaired drivers commonly involved a number of different tests.

THC is a psychoactive drug which can be detected in body fluids, such as saliva and blood, three to six hours after its consumption, and can be retained in the body for several days [18]. Unlike the roadside testing of alcohol in breath, there is no established rapid on-site screening method for detecting THC [19–21]. Current THC measurements in body fluids, such as blood, urine and saliva, are performed by centralized laboratories using classical methods and bulky instruments based on liquid chromatography, GC-MS and GC-MS with solid phase micro-extraction [22,23]. As cannabis may exist at measurable amount in the oral bio-fluid, and owing to its simple sample collection, saliva is one of the recommended matrices for detecting THC, and is highly suitable for rapid on-the-spot roadside tests [24–26]. Saliva-based THC detection is of particular interest for on-site screening, as it is a non-invasive method, and unlike blood assays, obviates the need for invasive sample collection [27]. The concentration of THC in saliva is a function of the time since the marijuana consumption [19], with a maximum salivary THC level of 16 μM observed 1–2 h after consuming the drug [28]. The ability to detect THC along with alcohol in the same saliva sample is of particular recent interest considering the synergistic effect of these drugs and the growing simultaneous recreational use of these substances.

Wearable electrochemical sensors are very promising tools to detect THC, as well as alcohol, in a timely and convenient manner. THC is an electroactive compound and its oxidation reaction was discussed earlier [29]. However, the electrochemical detection of THC is challenging due to its hydrophobic character [18]. To address this challenge and improve the THC solubility researchers have used different organic solvents prior to its voltametric detection using glassy carbon electrode [30]. Another electrochemical approach involved the preconcentration of THC onto a carbon-paste electrode sensor [29].

We have witnessed a tremendous recent interest in wearable sensors for on-body and on-site chemical detection [31–36]. Such wearable chemical sensors have recently been introduced in a variety of form factors, based on different clothing and accessories which can comfortably be worn on the body. While early efforts towards wearable chemical sensors have focused on healthcare and fitness monitoring, recent activity has led to the wearable devices for security and forensic applications [37–40]. We demonstrated recently a ring-based sensor platform for detecting explosives and nerve agents in liquid/vapor phases [40]. An oxygen saturation (SpO_2) sensor, embedded in a finger ring, has been developed by Sola et al. [41]. To the best of our knowledge, there are no reports on using wearable devices for detecting THC. On the other hand, wearable alcohol sensors have been demonstrated using sweat [42,43], saliva [44] and tears [45] biofluids, with good correlation to blood alcohol concentrations [46].

Herein, we demonstrate a ring-based sensor platform for the direct, rapid and simultaneous electrochemical detection of THC and alcohol in diluted saliva. The dual drug-of-abuse sensing ring cap offers direct square-wave voltammetric detection of THC along with amperometric (enzymatic) biosensing of alcohol, with no apparent cross talk, and high sensitivity down to 0.5 μM THC and 0.2 mM alcohol. The wearable ring body contains the embedded electronic board and enables a wireless data transmission. The board houses the potentiostatic circuitry, the microcontroller unit (MCU) and the antenna. Spring loaded pins are used to connect the printed circuit (embedded within the ring case), to the exposed current collectors of the sensing electrodes on the ring cap. Such alignment of spring-loaded pins allows rapid replacement of the sensor cover following each saliva assay. The resulting wearable THC/alcohol ring sensor holds considerable promise for on-the-spot roadside screening for drug-impaired driving and for alerting wearers about their own intoxication levels before driving. We hope that this activity will be extended to the use of wearable devices for detecting other major drugs of abuse.

2. Experimental

2.1. Chemicals and materials

Ag/AgCl ink (E2414) and carbon-Prussian blue (PB) ink (C2070424P2) were obtained from Gwent Inc. (Torfaen, UK). Carbon graphite ink (E3449) was obtained from Ercon Inc (Wareham, MA, USA). All inks were used as received. Polyethylene terephthalate (PET) was used as the substrate for fabrication of screen-printed electrodes. Analytical grade dipotassium hydrogen phosphate (K_2HPO_4), potassium dihydrogen phosphate (KH_2PO_4), sodium acetate, potassium chloride, ethanol, Δ^9-Tetrahydrocannabinol solution (1.0 mg/mL in methanol, analytical standard, for drug analysis), ethanol, chitosan, glutaraldehyde, multiwall carbon nano-tube and alcohol oxidase (AOx) from *Pichia pastoris* were obtained from Sigma-Aldrich (St. Louis, MO, USA). All reagents were used without further purification. For on-body measurements, a commercial Breathalyzer (BAC track(R) s80) was used to assess blood alcohol concentrations. All chemicals were of analytical grade and used without further purification. Ultrapure deionized water was used in the preparation of aqueous electrolyte solutions.

2.2. Screen-printed electrodes fabrication process

Screen printing was carried out by following our previous publications [40]. Briefly, a semi-automatic MMP-SPM screen printer (Speedline Technologies, Franklin, MA, USA) and custom stencils designed using AutoCAD software (Autodesk, San Rafael, CA) and produced by Metal Etch Services (San Marcos, CA, USA) using stainless steel stencils with dimensions of 12 × 12 inches were used. The alcohol biosensors were screen-printed on a flexible PET sheet through multiple steps. First, Ag/AgCl ink was used to prepare the reference electrode and the conductive trails used for the electrical connections. The printed sheet was then cured at 80 °C for 10 min. Subsequently, Carbon Prussian Blue (PB) ink was used to print the working electrode and the layer was cured at 75 °C for 10 min. Further, the working electrode was modified by drop casting method. For the alcohol biosensor, 3 μL of enzyme mixture (9:1 ratio of commercial AOx solution to 10 mg/mL BSA in PBS) was applied to the working electrode and allowed to dry at 4 °C for 2 h. Next, 2 μL of 0.5% chitosan was applied over the dried enzyme layer, followed by 0.5 μL of 2% glutaraldehyde, and the biosensor was dried at 4 °C overnight. The transparent insulator (Dupont 5036, Wilmington, DE) was used to define the electrode area. For preparation of THC sensor, 1% MWCNT was mixed with carbon ink and used for printing the working and counter electrodes.

2.3. Electrode interface and electronics

The developed sensor strip was connected to a small lab-made wearable wireless potentiostatic board which was developed on an FR-4 substrate, a composite material made of woven fibre glass cloth with an epoxy resin binder that is flame resistant. The board – embedded within the ring case - contained a SWV and amperometric circuit designed for three-electrode system: working (WE), counter (CE) and reference (RE) electrodes. The SWV circuit facilitates scanning potential excitation waveform controlled by a micro controller unit (MCU). The MCU functions to integrate an analog-to-digital converter (ADC) for the current measurements at the WE. Details on the functionality of ring board were described earlier [40] and further in the Results and Discussion section.

2.4. Electrochemical measurements

The square wave voltammetry (SWV) and amperometric experiments were carried out using a home-made wireless potentiostatic circuitry, embedded within the ring platform. The electrochemical system was set using a screen-printed four electrodes system (WE1,

WE2, RE and CE), which used Ag/AgCl as a joint reference electrode and carbon as joint counter electrode. For THC detection, SWV measurements were carried out at WE1 using electrode printed from 1% MWCNT modified carbon ink. The frequency, amplitude and E step were set as 20 Hz, 0.025V and 0.004 V, respectively, and the potential was scanned from 0 to +0.8V. For ethanol biosensing, PB/AOx modified carbon electrode was used as working electrode (WE2) along with amperometric measurements at an applied potential of −0.1V for 90 s for monitoring the reduction of the enzymatically generated peroxide. For each individual electrochemical measurement, 200 μL solution droplet was dispensed on to the electrode to cover the entire electrode surface of the ring cap. To establish the ethanol calibration curve, first, the baseline of the buffer (PBS) medium was recorded at least for five scans before spiking the ethanol over the 0.2–1 mM concentrations range with 0.2 mM increment. For THC detection, a freshly prepared 500 μM THC solution was used to construct a calibration curve. First, a stable, noise-free buffer baseline was recorded using SWV and subsequently for THC solutions over the 1–6 μM range, with 1 μM THC increments.

2.5. THC/alcohol detection in saliva

For the detection of THC and alcohol in saliva, different concentrations of both analytes were prepared. Saliva samples were collected immediately before analysis by spitting into a salivette tube and were centrifuged to 10,000 rpm for 2 min. Four different aliquots of centrifuged saliva were taken in four different Eppendorf tubes and were spiked with known THC concentrations between 10 and 40 μM. Next, these THC-spiked saliva samples were diluted 10-fold in PBS and assayed on the ring cap sensor. The same saliva collection protocol was used for alcohol detection. The collected saliva samples were divided into six vials and spiked with ethanol to prepare final concentrations ranging from 1 to 6 mM; these samples were subsequently diluted for 10 times to record the amperometric response. The analysis began with recording of baseline (saliva with no ethanol) until it was stable, followed by switching to the diluted saliva sample containing ethanol within the 0.1–0.6 mM range. The total time for the simultaneous alcohol and TCH detection was ~6 min, including 3 min for the saliva collection and treatment and 3 min for the alcohol and THC electrochemical measurements.

3. Results & discussion

3.1. Concept and mechanism of THC and alcohol ring sensor

The new dual-analyte THC/alcohol ring sensor system was realized using our previously described miniaturized ring potentiostatic board capable of performing SWV and chronoamperometry (CA) [40]. As illustrated in Fig. 1, the ring is composed primarily of three parts, a ring case, the electronic board and the sensor strip. The ring case is used to enclose the electronic board, which has wireless capabilities to carry out the voltammetric and amperometric measurements. The printed sensor electrodes on the ring cap were coupled to the electronic board (Fig. 1A). The unique connection system between the sensor and the ring board will be further discussed in Fig. 2. For the dual THC/alcohol detection in saliva, a screen-printed sensor layout was designed to resemble the cannabis plant leaves (Fig. 1Aa). The sensing system consists of 4 electrodes: two working electrodes ($WE1_{THC}$ and $WE2_{AOx}$ with exposed areas of 23 and 8 mm^2, respectively), the counter electrode (52 mm^2), and a Ag/AgCl reference electrode printed in between the two working electrodes (24 mm^2). The THC electrode was fabricated by using screen-printing of a carbon graphite ink (Ercon Inc) modified with MWCNT (1%). The THC detection was performed by SWV, while monitoring the THC oxidation over a potential window from 0V to +1.0V. The complete four-electrode sensor ring for detecting the THC and alcohol, worn on a human subject finger, is illustrated in Fig 1Ab and Ac shows the ring sensor structure with embedded electronic component along with the printed sensor strip with dual electrochemical modality (SWV and amperometry). THC is a phenolic molecule and its electrochemical behaviour resembles a typical phenolic voltammetric response [47–49], with a well-defined irreversible anodic peak current at +0.35 V (red curve), corresponding to a one-electron oxidation process shown in the reaction mechanism of Fig. 1B. The working electrode transducer for the alcohol biosensing was printed using Prussian Blue ink (Gwent Inc.), which was later modified with a bio-recognition layer of AOx/chitosan/glutaraldehyde [42]. The alcohol signal was recorded by monitoring the selective reduction of the hydrogen peroxide (H_2O_2) product of the AOx reaction at the Prussian Blue transducer (Fig. 1B right side). Such cathodic current signal is directly proportional to the ethanol concentration [45]. A typical chronoamperometric response to ethanol is shown in the schematic in Fig. 1B (in blue).

3.2. Electronic board design and integration for ring sensors

The marijuana-leaf shaped printed electrode layout has been connected to a miniaturized square-shaped potentiostat performing the SWV and CA operations. The small printed circuit board (PCB) was developed through the stacking of two electronic printed circuit boards. The wearable ring sensor platform is enabled with both electrochemical techniques SWV and CA (Fig. 1Ba). As illustrated in Fig. 2A, several steps were involved to fabricate the screen printed sensor strip, which sequentially included printing of a Ag/AgCl layer on PET substrate, then printing of carbon and Prussian blue layers, following by printing of the insulating layer to restrain the sensor diameter and define the active area and to protect the standing connectors. Fig. 1Ab illustrates a dual printed sensor array on PET while Fig. 2Ba shows the square-shaped skeleton of the developed electronic board (PCB) with its electronic circuitry components. This miniaturized ring board (15 × 15 mm^2) is capable of performing SWV and CA measurements independently. Fig. 2Bb depicts a microcontroller unit (MCU) used to control the SWV potential scanning between the WE and the RE. The applied potential can also be fixed for the chronomperometric operation. The controller unit integrates an analog-to-digital converter for calculating the current at the WE, and a Bluetooth Low Energy (BLE) host device, connected to a small chip antenna to enable the wireless communication to a smart host device. A custom designed graphical interface program using MATLAB operates the potentiostat wirelessly and transmits the electrochemical sensor outputs.

For the practicality of ring sensor, a quick connect mechanism has implemented to expedite the replacement of the used screen-printed electrodes. This mechanism relies on spring loaded pins (Harwin, P70-6000045) to connect the printed circuit board (PCB) in the body of the ring to the exposed SPE on the ring cap. The spring-loaded contacts are mounted on a custom printed circuit board (PCB) that aligns the pins with the current collectors of the SPE. The current collectors are extended to the backside of the SPE with conductive copper tape (3 M, 1181 Tape). This interface board provides soldering points for four wires on the opposite end of the assembly (Fig. 2C). The silicon glue is applied to the surface of the PCB to mount the interface board and to seal the electronics compartment. The wires were routed through the sealed compartment to the PCB and connected as needed for the measurements.

The miniaturized, wireless potentiostat served for performing the amperometric and SWV measurements of alcohol and THC, respectively. The system is implemented on two printed circuit boards which are stacked to reduce the total system size. The power is supplied by a +3.6V rechargeable Li-ion coin cell (PowerStream, LIR1620) which provides enough power to run continuous measurements for over 7h. The battery is mounted on the lower PCB along with the DC-DC regulators which provides stable supply and reference voltages for the circuit. The upper PCB contains the potentiostat circuit and the MCU

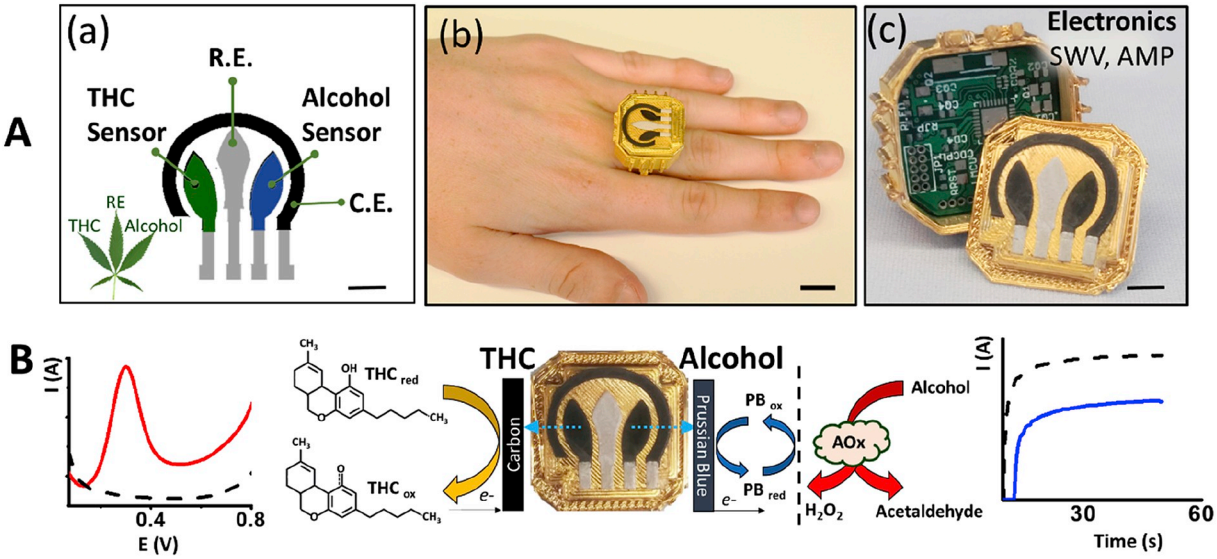

Fig. 1. (A) (a) Sensor design for simultaneous detection of THC and alcohol (scale bar 8 mm). (b) Real image of ring-based sensor platform embedded with marijuana designed sensor for detecting THC-alcohol (scale bar 15 mm). (c) Images showing a ring polymeric case with the integrated electronics and replaceable screen-printed electrodes based on (from left to right) a carbon modified with 1% MWCNT working electrode (WE 1), an Ag/AgCl reference electrode (RE), a carbon/Prussian-blue working electrode (WE 2), and a carbon counter electrode (CE) (scale bar 5 mm); (B) voltammograms of THC detection (in red) on W1 using ring sensor along with the THC oxidation mechanism, followed by alcohol detection mechanism using Prussian-blue modified sensor (W2); an amperogram of alcohol detection is illustrated (in blue). (For interpretation of the references to colour in this figure legend, the reader is referred to the Web version of this article.)

(Texas Instruments, CC2640). The MCU has an integrated Bluetooth Low Energy (BLE) radio which is used for all communication with the system. The potentiostat circuit relies on three operation amplifiers and a 2 channel, 16-bit DAC (Texas Instruments, DAC8563). The first amplifier is used to buffer the reference electrode. The high input impedance of the buffer reduces the current flowing through the reference electrode which helps to minimize polarization error. The second amplifier is the control amplifier and is configured with a feedback loop which compares the buffered reference and the control signal. This control signal is generated by one of the two output channels of the DAC and is used to set the potential of the electrochemical cell. The amplifier maintains the potential of the cell by sourcing or sinking the

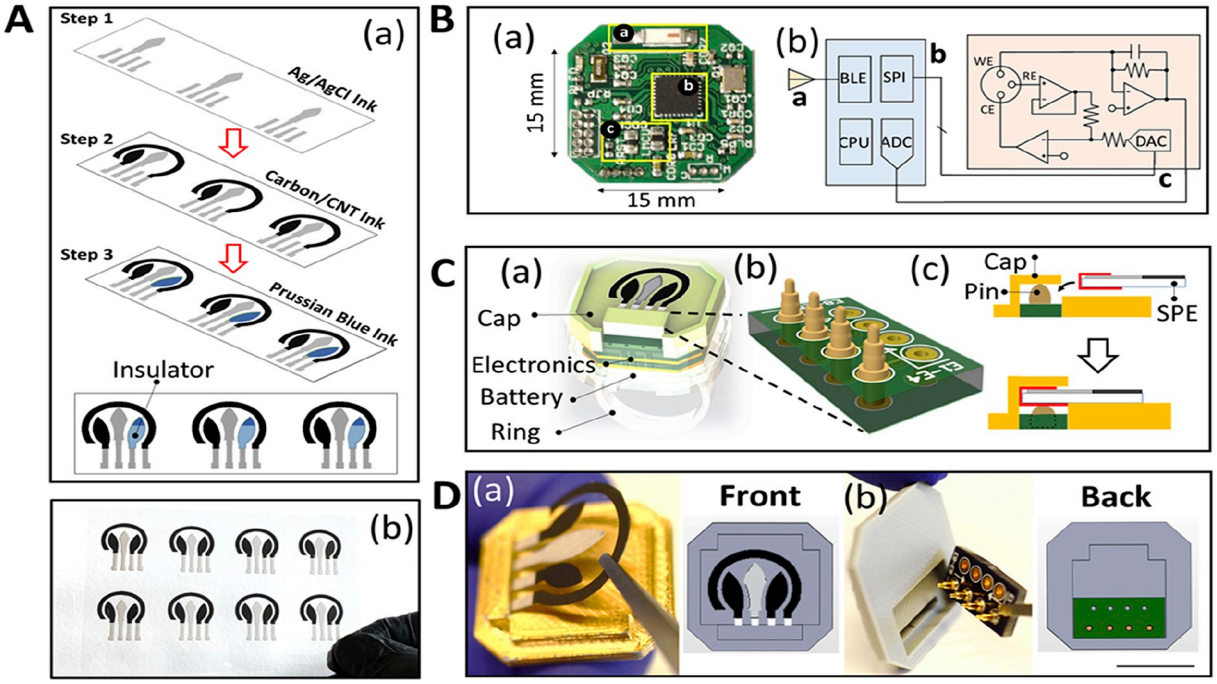

Fig. 2. Fabrication of ring-based wearable sensing platform with the screen-printed sensing electrodes and embedded electronic board for THC and alcohol detection. (A) (a) Screen-printing steps for fabricating the sensing electrodes: step 1, Ag/AgCl current collectors and RE electrode; step 2, Carbon/1% MWCNT WE 1 and CE; step 3, carbon-Prussian blue WE 2, final assembly with blue insulator and (b) image of sensor array. (B) (a) Image of the ring PCB showing, a, antenna, b MCU, c potentiostat (on reverse side), and (b) block diagram illustrating the main subsystems - antenna, MCU, and potentiostat circuit. (C) (a) 3D model of the system with integrated SPE and PCB. (b) Detailed view of SPE interface board showing the spring-loaded SPE contacts, (c) insertion of the SPE, (D) (a) placement of SPE on ring (front side), and (b) mounting of the interface board (back side). Scale bar: 15 mm. (For interpretation of the references to colour in this figure legend, the reader is referred to the Web version of this article.)

appropriate amount of current. The third operational amplifier is configured as a transimpedance amplifier and converts the electrochemical current into a measurable voltage. The second DAC channel is used to generate a bias voltage for the control and transimpedance amplifiers. Adjusting this voltage allows tailoring of the measurement range of the system for each analyte.

To start a measurement, a BLE command is sent to the wearable system from the MATLAB user interface. This interface is used to establish a BLE connection with the potentiostat, configure the measurement parameters, and display the results. After receiving the configuration packets, the MCU generates two digital codes which are representative of the control and bias signals. These codes are sent to the 16-bit DAC which then updates the outputs to requested bias and analog control voltages. In a SWV measurement, the control signal is a superposition of a square wave and a staircase waveform. The 16-bit DAC used in this application provides the required resolution to create a high resolution SWV waveform. For the amperometric measurements, this control signal is constant potential. Regardless of the technique, the control signal is fed into the potentiostat circuitry to set the potential between the working and reference electrodes. The change in potential disrupts the equilibrium of the electrochemical cell and causes current to flow between the counter and working electrodes. The potentiostat then filters, amplifies, and converts this current into a voltage with a transimpedance amplifier. This voltage is routed to the MCU where it is sampled by an integrated 12-bit analog to digital converter. In a SWV measurement the signal is sampled on both the rising and falling edge of the square wave. This sampling technique measures both the forward and reverse currents to minimize the impact of the non-faradic current. The final current is the difference between these two currents. In an amperometric experiment, the current is sampled at the constant rate configured in the MATLAB interface. The sampled data is then transmitted over BLE to the MATLAB interface where it is plotted for analysis. This process is repeated for the duration of the measurement. The integration of electronic board and printed sensors on ring sensor (top view of electrode placement) is illustrated in Fig. 2Da, and then the front view is shown. Later, the integration of pins to the ring sensor at the back is presented.

3.3. THC and alcohol detection

SWV and amperometry techniques were used for detecting THC and alcohol, respectively, in PBS and diluted saliva. For THC analysis, SWV measurements were carried out for initial optimization of potential, scan rate, frequency and incubation time. Once the experimental parameters were optimized, the THC calibration studies were performed using 1% MWCNT modified carbon screen printed electrodes with a marijuana design. Since the THC solution was prepared in methanol, it is necessary to test the response of methanol first. Hence, a control experiment was performed by simply testing methanol (3.2 μM). Fig. S1 shows no interference when testing the methanol present in the highest THC concentration (3.18 mM). Following optimization and control tests, a calibration curve was built for THC in PBS. Fig. 3a shows the typical anodic SWV scans obtained for THC in buffer solution containing increasing THC levels in the range 1–6 μM, with 1 μM increments. This series displays good reproducibility and repeatability between the electrodes with a RSD of 2.23%. Such SWV response increases linearly with each THC addition (Fig. 3a linear graph). Using our printed 1% MWCNT/carbon ring-cap electrode allows convenient and sensitive detection of cannabis with a defined SWV peak at +0.3 V, even for THC concentrations as low as 0.25 μM (Fig. S2). After establishing the THC response and obtaining the calibration curve in buffer solution using ring-based sensor platform, five different strip sensors were used to assess the reproducibility and repeatability of the sensor in connection to 2 μM THC solutions. As illustrated in the Fig. 3Ab, the different printed electrodes display reproducible square-wave voltammograms with favourable signal-to-noise characteristics. The current response was recorded and plotted with their current values *vs* number of sensors tested (Fig. 3Ab, right). This plot reflects the similar current values and good repeatability with their current responses (RSD 2.67%, figure in the right; n = 3). The ethanol response and concentration dependence were established independently on the second enzyme-modified ring-cap working electrode, before testing of real saliva samples. As demonstrated in Fig. 3Ba, such ethanol detection was performed over the 0.1–1 mM range (with 0.1 mM increments) using AOx-modified Prussian-blue sensors (Fig. 3Ba). The amperometric ethanol biosensor displayed a very good response to these 0.1 mM additions, with favourable S/B characteristics. The resulting calibration plot, shown on the right side of Fig. 3Ba, is highly linear up to 0.8 mM, and start to level off at higher concentration. The reproducibility of different ethanol ring sensors is evaluated in Fig. 3Bb which displays 5 different amperograms for the biosensing of ethanol at the different sensors. A highly reproducible response with a RSD of 1.5% (n = 5) is obtained, as indicated from the corresponding plot (shown on the right side of Fig. 3Bb). Such repeatability test confirms the reliance of the Prussian-blue surface printing and modification with the AOx layer.

The ability of the system to detect ethanol and THC simultaneously in the same solution was also studied. Fig. 3C examines the cross talk of the neighbouring THC and alcohol sensors using the detection of ethanol followed by THC measurements in the same PBS solution. Recording the PBS base-line amperometric response (Fig. 3Ca) was followed by the addition of 0.8 mM ethanol (Fig. 3Cb, solid line). Subsequently, a SWV was recorded on the THC sensor (Fig. 3Cc), followed by the addition of 4 μM of THC (Fig. 3Cd). These results clearly indicate that the presence of 0.8 mM ethanol has no effect upon the SWV THC response.

3.4. THC and alcohol detection in saliva

Saliva is a challenging bio-fluid to perform direct electrochemical analysis due to considerable amounts of serous or mucous fluid in its composition, which makes saliva very viscous [33]. The high viscosity and presence of macromolecules can impair the electron transfer processes and hinder the electroanalytical performance. This challenge has been addressed here by diluting the saliva, a rapid step suitable for on-the-spot testing that minimizes the saliva viscosity (Fig. S3). Initially, the whole saliva was tested as matrix to spiked THC and alcohol molecules, interestingly; only alcohol displayed a favourable performance in whole saliva (Fig. S3a), while no THC peak was observed (Fig. S3d). The best dilution ratio for detecting both compounds simultaneously was found to be 1:10 (saliva: PBS).

Calibration of the alcohol ring sensor was performed in diluted saliva samples collected according with the procedure reported in the experimental section and illustrate in Fig. 4A. The obtained data shows a very stable and smooth response of alcohol concentration in a linear manner throughout the range of 0.1 mM–0.6 mM. In a similar way, THC calibration was also performed in saliva samples. For THC detection, WE1 was used, and it was modified by 1% MWCNT mixed in carbon ink before printing. As illustrated in Fig. 4Bb, THC was tested over the 0.1–0.4 μM concentration range. A clean and smooth baseline was recorded before the THC analysis, indicating no interference from the saliva constituents. The whole saliva samples were first spiked with 1–4 μM THC and subsequently diluted 10 times in buffer. Interestingly, a distinct THC oxidation peak was obtained and recorded at +0.42V. The related current values were plotted against THC concentration and illustrated in Fig. 4Bb, as linear curve. Fig. 4C illustrated the cross-talk studies performed in diluted saliva samples to evaluate the effect of both molecules during their respective detection in real matrix. Initially, the saliva (1:10) baseline was recorded (Fig. 4Ca), followed by the addition and amperometric measurement of 0.8 mM ethanol (Fig. 4Cb, solid line). In the same saliva solution containing the 0.8 mM ethanol, a SWV was performed (Fig. 4Cc) followed by the addition of 4 μM THC (Fig. 4Cd). As we can observe, there was no cross talking in

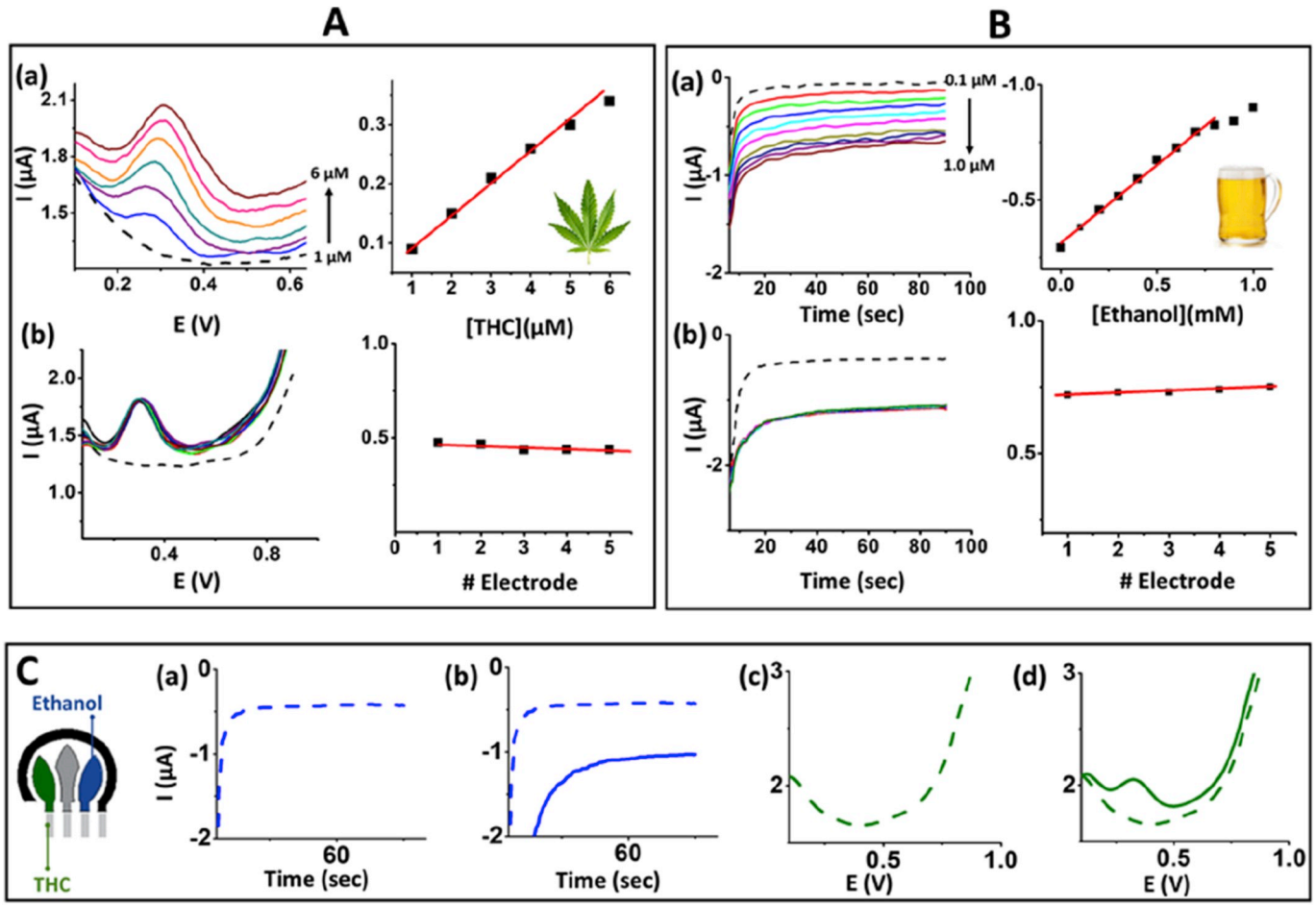

Fig. 3. In vitro detection of THC and ethanol. (A); (a) Square wave voltammograms (frequency, 20 Hz, amplitude 25 mV, E step, 4 mV) for the oxidation of THC in PBS (0.1 M, pH 7.4) in the range 1–6 μM (1 μM increment) using 1% MWCNT: Ercon carbon printed electrode. On the right side, the respective current values obtained from THC oxidation , range 1–6 μM. Incubation time was 1 min. b) SWV response to 2 μM THC recorded using five different sensors (reproducibility of the sensor performance) with their respective current responses (right side) (B) a) Alcohol response from 0.1 to 1 μM with 0.1 μM additions using AOx-modified Prussian-blue sensor (W2); applied potential, −0.1V and respective calibration plot (right side)(b) Amperometric response for 1 mM EtOH recorded using five different sensors, with the resulting current signals showing a good reproducibility among tested sensors (righ side). (C) In-vitro cross-talk evaluation of the alcohol/THC sensor. The voltametric response of (a) PBS (dotted line) (b) PBS and 0.8 mM (solid blue curve) ethanol followed by the (c) SWV of PBS containing the previously added 0.8 mM ethanol (dotted green line) and consecutive adition of (d) 4 μM THC (solid green line). (For interpretation of the references to colour in this figure legend, the reader is referred to the Web version of this article.)

the THC measurement following the ethanol detection. It is important to notice that the cross talking of measuring ethanol after THC measurement could not be performed as the THC solution contained dissolved methanol; however, in real scenario this would not be an issue once THC is not dissolved in methanol in human saliva.

The performance of the wearable THC-ethanol platform was evaluated using real saliva samples. The system was tested first after alcohol consumption in order to evaluate the ability of the sensor in measuring relevant salivary ethanol concentrations after 1:10 dilution. Fig. 4D illustrates the procedure employed for such decentralized ethanol testing. The volunteer was asked first to consume 100 mL of alcoholic beverage (19.5% Alc./Vol.), and saliva was collected every 10 min after measuring the blood alcohol concentration (BAC) with a commercial breathalyser. Fig. 4Db shows the CA of the several BACs where the black amperogram corresponds to the saliva sample before drinking. It can be observed that the sensor was able to successfully detect the BAC variations following such 10-fold dilution of saliva in PBS. Using the saliva corresponding to BAC 0.039% (Fig. 4Ea) a SWV baseline was obtained, followed by the addition of 1 μM and 2 μM THC (Fig. 4Eb). The corresponding voltammograms display distinct THC peak currents for both concentrations, illustrating the ability to detect THC in real sample containing physiological ethanol levels.

4. Conclusions

Alcohol and cannabis are often used in combination, and their combined synergistic effects may greatly increase the risk of fatal accidents. To address these risks, we have presented a sensor ring concept, based on embedding a powerful wireless electronic board into a ring platform, along with a printed dual-sensor electrode cap, for the simultaneous field detection of salivary THC and alcohol. The attractive capabilities of the new wearable sensor ring system have been demonstrated for sensitive and rapid voltammetric and amperometric measurements of salivary THC and alcohol, respectively. The THC ring sensor offers a detection limit of 0.5 μM, which is suitable for detecting salivary THC even 24 h after the marijuana consumption [28]. Both electrochemical techniques have been executed using the potentiostatic circuitry embedded within the ring body. Such ring-based integration of miniaturized wireless electronic interface facilitates selective “on the spot” detection of cannabis and alcohol with no cross talk or false alarms. The ring platform allows rapid replacement of the disposable dual sensor strip, with the sensor strips having high storage stability when considering the stability of the immobilized alcohol-oxidase enzyme. Additional sensors, such as pH and temperature, could be readily integrated into the ring platform for addressing temperature changes or

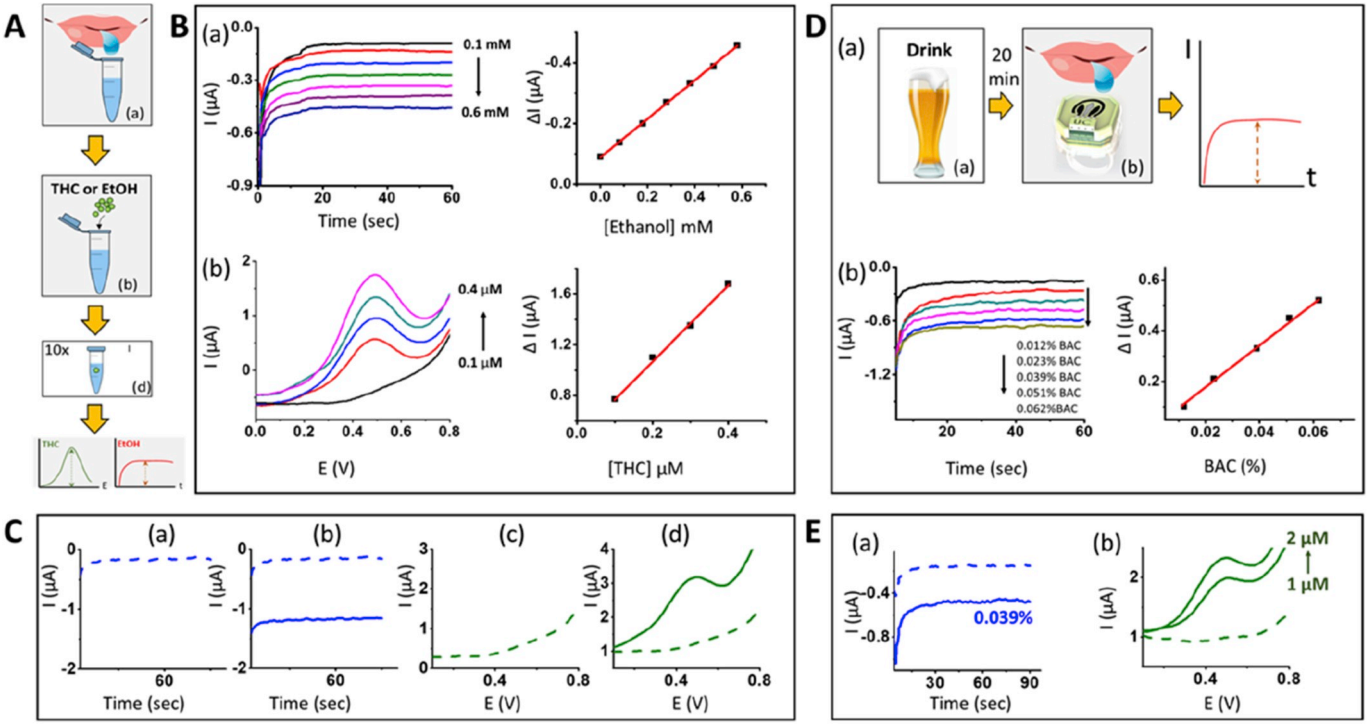

Fig. 4. THC-alcohol detection in Saliva samples. (A) Schematic illustration of saliva collection using Salivette tube (a), followed by the addition of THC-alcohol (b), and dilution and then detection (c) using ring-based sensor platform. (B) (a) amperometric response of the ethanol (0.1–0.6 mM) in real diluted saliva (1:10) and obtained current values of 1:10 diluted saliva spiked with ethanol (right side). (b) SWV response of THC spiked in 1:10 diluted saliva samples and corresponding current values as linear graph (righ side). (C) Cross-talk evaluation of the alcohol/THC sensor. Amperometric response of (a) 1:10 diluted saliva in PBS; (b) diluted saliva (1:10) and 0.8 mM ethanol response (solid line); (c) SWV of 1:10 diluted saliva containing the 0.8 mM spiked ethanol, followed by (d) spiking 4 μM THC (solid line). Dotted lines are the baseline recorded for both ethanol and THC. SWV for the oxidation of THC in PBS (0.1 M, pH 7.4); ethanol measurements were performed using an applied potential of −0.1V for 100 s. (D) (a) Procedure used for collecting saliva samples after consuming wine and detection using ring sensor. (b) Amperometric response of ethanol in real diluted saliva before consuming wine (black, BAC 0.00%) and after the wine consumption (in red, 0.012%, in green, BAC 0.023%, in magenta, BAC 0.039%, in blue, BAC 0.051% and in brown, 0.062%) and respective current values (right side). Conditions: Square wave voltametric measurements of the THC oxidation in PBS (0.1 M, pH 7.4); for ethanol, the applied potential was −0.1V for 100 s. (E) (a) Response of 1:10 diluted saliva samples before (dotted line) and at BAC level of 0.039%. , followed by (b) SWV of the saliva containing alcohol (dotted line) and same sample spiked with THC at 1 and 2 μM. SWV conditions, as in Fig. 3. (For interpretation of the references to colour in this figure legend, the reader is referred to the Web version of this article.)

variations in the saliva pH. The new wearable sensing concept can be readily expanded for the monitoring of other drugs of abuse. The new wearable platform thus holds considerable promise for rapid roadside testing of drivers suspected of driving under the influence of alcohol and/or drugs. We also expect that additional wearable chemical sensors will be incorporated in the near future into rings or other accessories which can be worn comfortably on the body.

CRediT authorship contribution statement

Rupesh K. Mishra: Methodology, Investigation, Data curation, Writing - original draft, Writing - review & editing. **Juliane R. Sempionatto:** Methodology, Conceptualization, Investigation, Visualization, Writing - original draft, Writing - review & editing. **Zhanhong Li:** Methodology, Investigation. **Christopher Brown:** Software, Writing - original draft. **Nathalia M. Galdino:** Investigation, Writing - original draft. **Rushabh Shah:** Investigation. **Shuyang Liu:** Investigation. **Lee J. Hubble:** Methodology, Investigation. **Kara Bagot:** Conceptualization. **Susan Tapert:** Conceptualization. **Joseph Wang:** Conceptualization, Resources, Project administration, Visualization, Supervision, Writing - review & editing.

Declaration of competing interest

The authors declare no competing financial interest.

Acknowledgements

Financial support from The Defence Threat Reduction Agency Joint Science and Technology Office for Chemical and Biological Defence (HDTRA 1-16-1-0013) and the UCSD Centre of Wearable Sensors is acknowledged. J.R.S. acknowledges support from the National Council for Scientific and Technological Development (CNPq-216981/2014-0). R.K.M. acknowledges a fellowship from Department of Biotechnology, New Delhi, India. N.M.G. acknowledges CAPES scholarship/PDSE/ number 88881.188746/2018–01. L.J.H. acknowledges support from the Research Plus Julius Career Award by CSIRO and Z.L. acknowledges support from the 2018 Shanghai Young and Middle-aged Teachers' Foreign Visiting Program.

Appendix A. Supplementary data

Supplementary data to this article can be found online at https://doi.org/10.1016/j.talanta.2020.120757.

References

[1] R.A. Zucker, S.A. Brown, The Oxford Handbook of Adolescent Substance Abuse, Oxford University Press, 2019, https://doi:10.1093/oxfordhb/9780199735662.001.0001.
[2] B.C. Foster, H. Abramovici, C.S. Harris, Cannabis and cannabinoids: kinetics and interactions, Am. J. Med. 132 (2019) 1266–1270, https://doi.org/10.1016/j.amjmed.2019.05.017.
[3] O.H. Drummer, D. Gerostamoulos, N.W. Woodford, Cannabis as a cause of death: a

review, Forensic Sci. Int. 298 (2019) 298–306, https://doi.org/10.1016/j.forsciint.2019.03.007.
[4] J. Bierhoff, R. Haardörfer, M. Windle, C.J. Berg, Psychological risk factors for alcohol, cannabis, and various tobacco use among Young adults: a longitudinal analysis, Subst. Use & Misuse 54 (2019) 1365–1375, https://doi.org/10.1080/10826084.2019.1581220.
[5] R.N. Lipari, A. Hughes, J. Bose, Driving under the Influence of Alcohol and Illicit Drugs, Substance Abuse and Mental Health Services Administration (US), (2013) http://www.ncbi.nlm.nih.gov/pubmed/28252900 , Accessed date: 18 September 2019.
[6] Alcohol-impaired driving (n.d.), https://crashstats.nhtsa.dot.gov/Api/Public/ViewPublication/811155 , Accessed date: 18 September 2019.
[7] J.M. Walsh, R. Flegel, L.A. Cangianelli, R. Atkins, C.A. Soderstrom, T.J. Kerns, Epidemiology of alcohol and other drug use among motor vehicle crash victims admitted to a trauma center, Traffic Inj. Prev. 5 (2004) 254–260, https://doi.org/10.1080/15389580490465319.
[8] W. Hall, L. Degenhardt, Adverse health effects of non-medical cannabis use, Lancet 374 (2009) 1383–1391, https://doi.org/10.1016/S0140-6736(09)61037-0.
[9] NIDA InfoFacts: drugged driving (n.d.), https://www.mentalhelp.net/addiction/what-is-it/drugged-driving/ , Accessed date: 18 September 2019.
[10] W. Hall, Acute cannabis consumption and motor vehicle collision risk: systematic review of observational studies and meta-analysis, BMJ 344 (2012) e1735, https://doi.org/10.1136/sbmj.e1735.
[11] R.L. Hartman, M.A. Huestis, Cannabis effects on driving skills, Clin. Chem. 59 (2013) 478–492, https://doi.org/10.1373/clinchem.2012.194381.
[12] Fatal road crashes involving marijuana double after state legalizes drug: foundation research also shows that legal limits for marijuana and driving are meaningless - ScienceDaily (n.d.), https://www.sciencedaily.com/releases/2016/05/160510103131.htm , Accessed date: 18 September 2019.
[13] R.A. Sewell, J. Poling, M. Sofuoglu, The effect of cannabis compared with alcohol on driving, Am. J. Addict. 18 (2009) 185–193, https://doi.org/10.1080/10550490902786934.
[14] M.S. Subbaraman, W.C. Kerr, Simultaneous versus concurrent use of alcohol and cannabis in the national alcohol survey, alcohol, Clin. Exp. Res. 39 (2015) 872–879, https://doi.org/10.1111/acer.12698.
[15] S.A. Meda, R.V. Gueorguieva, B. Pittman, R.R. Rosen, F. Aslanzadeh, H. Tennen, S. Leen, K. Hawkins, S. Raskin, R.M. Wood, C.S. Austad, A. Dager, C. Fallahi, G.D. Pearlson, Longitudinal influence of alcohol and marijuana use on academic performance in college students, PLoS One 12 (2017) e0172213, , https://doi.org/10.1371/journal.pone.0172213.
[16] M. Marillier, A.G. Verstraete, Driving under the influence of drugs, Wiley Interdiscip. Rev. Forensic Sci. 1 (2019) e1326, https://doi.org/10.1002/wfs2.1326.
[17] P. Pacher, S. Bátkai, G. Kunos, The endocannabinoid system as an emerging target of pharmacotherapy, Pharmacol. Rev. 58 (2006) 389–462, https://doi.org/10.1124/pr.58.3.2.
[18] M.A. Huestis, Human cannabinoid pharmacokinetics, Chem. Biodivers. 4 (2007) 1770–1804, https://doi.org/10.1002/cbdv.200790152.
[19] S.C.D. Dobri, A.H. Moslehi, T.C. Davies, Are oral fluid testing devices effective for the roadside detection of recent cannabis use? A systematic review, Public Health 171 (2019) 57–65, https://doi.org/10.1016/J.PUHE.2019.03.006.
[20] S.I. Hwang, N.G. Franconi, M.A. Rothfuss, K.N. Bocan, L. Bian, D.L. White, S.C. Burkert, R.W. Euler, B.J. Sopher, M.L. Vinay, E. Sejdic, A. Star, Tetrahydrocannabinol detection using semiconductor-enriched single-walled carbon nanotube chemiresistors, ACS Sens. 4 (2019) 2084–2093, https://doi.org/10.1021/acssensors.9b00762.
[21] A. Voss, K. Witt, T. Kaschowitz, W. Poitz, A. Ebert, P. Roser, K.-J. Bär, Detecting cannabis use on the human skin surface via an electronic nose system, Sensors (Basel). 14 (2014) 13256–13272, https://doi.org/10.3390/s140713256.
[22] S. Malaca, F.P. Busardò, M. Gottardi, S. Pichini, E. Marchei, Dilute and shoot ultra-high performance liquid chromatography tandem mass spectrometry (UHPLC–MS/MS) analysis of psychoactive drugs in oral fluid, J. Pharm. Biomed. Anal. 170 (2019) 63–67, https://doi.org/10.1016/J.JPBA.2019.02.039.
[23] K. Purschke, S. Heinl, O. Lerch, F. Erdmann, F. Veit, Development and validation of an automated liquid-liquid extraction GC/MS method for the determination of THC, 11-OH-THC, and free THC-carboxylic acid (THC-COOH) from blood serum, Anal. Bioanal. Chem. 408 (2016) 4379–4388, https://doi.org/10.1007/s00216-016-9537-5.
[24] H. Stevenson, A. Bacon, K.M. Joseph, W.R.W. Gwandaru, A. Bhide, D. Sankhala, V.N. Dhamu, S. Prasad, A rapid response electrochemical biosensor for detecting thc in saliva, Sci. Rep. 9 (2019) 12701, https://doi.org/10.1038/s41598-019-49185-y.
[25] C. Wanklyn, D. Burton, E. Enston, C.A. Bartlett, S. Taylor, A. Raniczkowska, M. Black, L. Murphy, Disposable screen printed sensor for the electrochemical detection of delta-9-tetrahydrocannabinol in undiluted saliva, Chem. Cent. J. 10 (2016) 1, https://doi.org/10.1186/s13065-016-0148-1.
[26] J.-R. Lee, J. Choi, T.O. Shultz, S.X. Wang, Small molecule detection in saliva facilitates portable tests of marijuana abuse, Anal. Chem. 88 (2016) 7457–7461, https://doi.org/10.1021/acs.analchem.6b01688.
[27] M.A. Huestis, M.L. Smith, Cannabinoid markers in biological fluids and tissues: revealing intake, Trends Mol. Med. 24 (2018) 156–172, https://doi.org/10.1016/j.molmed.2017.12.006.
[28] R.S. Niedbala, K.W. Kardos, D.F. Fritch, S. Kardos, T. Fries, J. Waga, J. Robb, E.J. Cone, Detection of marijuana use by oral fluid and urine analysis following single-dose administration of smoked and oral marijuana, J. Anal. Toxicol. 25 (2001) 289–303, https://doi.org/10.1093/jat/25.5.289.
[29] R. Nissim, R.G. Compton, Absorptive stripping voltammetry for cannabis detection, Chem. Cent. J. 9 (2015) 41, https://doi.org/10.1186/s13065-015-0117-0.
[30] M.A. Balbino, I.C. Eleoterio, M.F. de Oliveira, B.R. McCord, Electrochemical study of delta-9-tetrahydrocannabinol by cyclic voltammetry using screen printed electrode, improvements in forensic analysis, Sens. Transducers 207 (2016) 73–78.
[31] J. Kim, A.S. Campbell, B.E. Ávila, J. Wang, Wearable biosensors for healthcare monitoring, Nat. Biotechnol. 37 (2019) 389–406, https://doi.org/10.1038/s41587-019-0045-y.
[32] A.K. Yetisen, J.L. Martinez-Hurtado, B. Ünal, A. Khademhosseini, H. Butt, Wearables in medicine, Adv. Mater. 30 (2018) 1706910, , https://doi.org/10.1002/adma.201706910.
[33] W. Gao, S. Emaminejad, H.Y.Y. Nyein, S. Challa, K. Chen, A. Peck, H.M. Fahad, H. Ota, H. Shiraki, D. Kiriya, D.H. Lien, G.A. Brooks, R.W. Davis, A. Javey, Fully integrated wearable sensor arrays for multiplexed in situ perspiration analysis, Nature 529 (2016) 509–514, https://doi.org/10.1038/nature16521.
[34] A.J. Bandodkar, W.J. Jeang, R. Ghaffari, J.A. Rogers, Wearable sensors for biochemical sweat analysis, Annu. Rev. Anal. Chem. 12 (2019) 1–22, https://doi.org/10.1146/annurev-anchem-061318-114910.
[35] W. Jia, A.J. Bandodkar, G. Valdés-Ramírez, J.R. Windmiller, Z. Yang, J. Ramírez, G. Chan, J. Wang, Electrochemical tattoo biosensors for real-time noninvasive lactate monitoring in human perspiration, Anal. Chem. 85 (2013) 6553–6560, https://doi.org/10.1021/ac401573r.
[36] A.M.V. Mohan, J.R. Windmiller, R.K. Mishra, J. Wang, Continuous minimally-invasive alcohol monitoring using microneedle sensor arrays, Biosens. Bioelectron. 91 (2017) 574–579, https://doi.org/10.1016/j.bios.2017.01.016.
[37] R.K. Mishra, A.M. Vinu Mohan, F. Soto, R. Chrostowski, J. Wang, A microneedle biosensor for minimally-invasive transdermal detection of nerve agents, Analyst 142 (2017) 918–924, https://doi.org/10.1039/C6AN02625G.
[38] A. Barfidokht, R.K. Mishra, R. Seenivasan, S. Liu, L.J. Hubble, J. Wang, D.A. Hall, Wearable electrochemical glove-based sensor for rapid and on-site detection of fentanyl, Sens. Actuators B Chem. 296 (2019) 126422, , https://doi.org/10.1016/J.SNB.2019.04.053.
[39] R. Cánovas, M. Parrilla, P. Mercier, F.J. Andrade, J. Wang, Balloon-embedded sensors withstanding extreme multiaxial stretching and global bending mechanical stress: towards environmental and security monitoring, Adv. Mater. Technol. 1 (2016) 1600061, , https://doi.org/10.1002/admt.201600061.
[40] J.R. Sempionatto, R.K. Mishra, A. Martín, G. Tang, T. Nakagawa, X. Lu, A.S. Campbell, K.M. Lyu, J. Wang, Wearable ring-based sensing platform for detecting chemical threats, ACS Sens. 2 (2017) 1531–1538, https://doi.org/10.1021/acssensors.7b00603.
[41] J. Sola, S. Castoldi, O. Chetelat, M. Correvon, S. Dasen, S. Droz, N. Jacob, R. Kormann, V. Neumann, A. Perrenoud, P. Pilloud, C. Verjus, G. Viardot, SpO2 sensor embedded in a finger ring: design and implementation, 28th IEEE, 2006, pp. 4295–4298, , https://doi.org/10.1109/IEMBS.2006.260820.
[42] J. Kim, I. Jeerapan, S. Imani, T.N. Cho, A. Bandodkar, S. Cinti, P.P. Mercier, J. Wang, Noninvasive alcohol monitoring using a wearable tattoo-based iontophoretic-biosensing system, ACS Sens. 1 (2016) 1011–1019, https://doi.org/10.1021/acssensors.6b00356.
[43] J. Kim, J.R. Sempionatto, S. Imani, M.C. Hartel, A. Barfidokht, G. Tang, A.S. Campbell, P.P. Mercier, J. Wang, Simultaneous monitoring of sweat and interstitial fluid using a single wearable biosensor platform, Adv. Sci. 5 (2018) 1800880, , https://doi.org/10.1002/advs.201800880.
[44] Y. Jung, J. Kim, O. Awofeso, H. Kim, F. Regnier, E. Bae, Smartphone-based colorimetric analysis for detection of saliva alcohol concentration, Appl. Opt. 54 (2015) 9183–9189, https://doi.org/10.1364/AO.54.009183.
[45] J.R. Sempionatto, L.C. Brazaca, L. García-Carmona, G. Bolat, A.S. Campbell, A. Martin, G. Tang, R. Shah, R.K. Mishra, J. Kim, V. Zucolotto, A. Escarpa, J. Wang, Eyeglasses-based tear biosensing system: non-invasive detection of alcohol, vitamins and glucose, Biosens. Bioelectron. 137 (2019) 161–170, https://doi.org/10.1016/J.BIOS.2019.04.058.
[46] A.S. Campbell, J. Kim, J. Wang, Wearable electrochemical alcohol biosensors, Curr. Opin. Electrochem. 10 (2018) 126–135, https://doi.org/10.1016/j.coelec.2018.05.014.
[47] M. Renaud-Young, R.M. Mayall, V. Salehi, M. Goledzinowski, F.J.E. Comeau, J.L. MacCallum, V.I. Birss, Development of an ultra-sensitive electrochemical sensor for Δ 9 -tetrahydrocannabinol (THC) and its metabolites using carbon paper electrodes, Electrochim. Acta 307 (2019) 351–359, https://doi.org/10.1016/j.electacta.2019.02.117.
[48] M. Gattrell, D.W. Kirk, A study of electrode passivation during aqueous phenol electrolysis, J. Electrochem. Soc. 140 (1993) 903–911, https://doi.org/10.1149/1.2056225.
[49] M.A. Balbino, M.M.T. de Menezes, I.C. Eleotério, A.A. Saczk, L.L. Okumura, H.M. Tristão, M.F. de Oliveira, Voltammetric determination of Δ9-THC in glassy carbon electrode: an important contribution to forensic electroanalysis, Forensic Sci. Int. 221 (2012) 29–32, https://doi.org/10.1016/j.forsciint.2012.03.020.